AD-A056 899 TEXAS TECH UNIV LUBBOCK DEPT OF ELECTRICAL ENGINEERING F/G 17/2
RADIO PROPAGATION VIA TRANSPONDER.(U)
MAY 78 T F TROST, P E GARRISON AFOSR-77-3374

UNCLASSIFIED AFOSR-TR-78-1196 NL

1 OF 1
AD
A056 899

END
DATE
FILMED
9-78
DDC

LEVEL II

(2)

RADIO PROPAGATION VIA TRANSPONDER

by
Thomas F. Trost
Paul E. Garrison

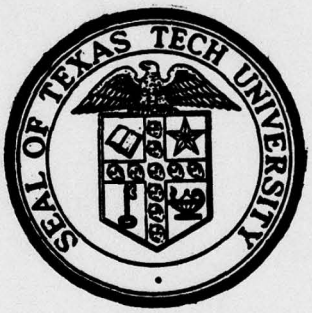

Final Technical Report on
Grant No. AFOSR 77-3374

May 1978

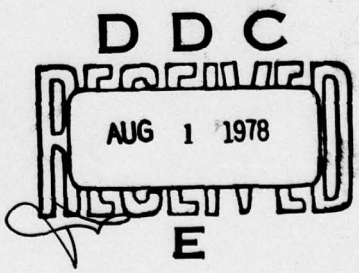

Department of Electrical Engineering
TEXAS TECH UNIVERSITY
Lubbock, Texas 79409

Unclassified

SECURITY CLASSIFICATION OF THIS PAGE (When Data Entered)

REPORT DOCUMENTATION PAGE

READ INSTRUCTIONS BEFORE COMPLETING FORM

1. REPORT NUMBER AFOSR-TR-78-1196	2. GOVT ACCESSION NO.
	3. RECIPIENT'S CATALOG NUMBER
4. TITLE (and Subtitle) RADIO PROPAGATION VIA TRANSPONDER.	5. TYPE OF REPORT & PERIOD COVERED Final rept. 1 Mar 77-Mar 78.
	6. PERFORMING ORG. REPORT NUMBER
7. AUTHOR(s) Thomas F. Trost, Paul E. Garrison	8. CONTRACT OR GRANT NUMBER(s) AFOSR-77-3374
9. PERFORMING ORGANIZATION NAME AND ADDRESS Department of Electrical Engineering, Texas Tech University, Lubbock, Texas 79409	10. PROGRAM ELEMENT, PROJECT, TASK AREA & WORK UNIT NUMBERS 2301/A1 61102F A1
11. CONTROLLING OFFICE NAME AND ADDRESS Air Force Office of Scientific Research, Bolling AFB, D.C. 20332 NP	12. REPORT DATE May 78
	13. NUMBER OF PAGES 55
14. MONITORING AGENCY NAME & ADDRESS (if different from Controlling Office) 57p.	15. SECURITY CLASS. (of this report) Unclassified
	15a. DECLASSIFICATION/DOWNGRADING SCHEDULE

16. DISTRIBUTION STATEMENT (of this Report)

Approved for public release; distribution unlimited

17. DISTRIBUTION STATEMENT (of the abstract entered in Block 20, if different from Report)

18. SUPPLEMENTARY NOTES

19. KEY WORDS (Continue on reverse side if necessary and identify by block number)

Radio propagation
UHF communications

20. ABSTRACT (Continue on reverse side if necessary and identify by block number)

A UHF radio propagation experiment was carried out over the southwestern U.S. in July, 1977. Radio signals were relayed between ground stations located up to 500 mi. (800 km.) apart by a parachute-borne transponder. The strength of the received signals was found to be in general agreement with calculations utilizing standard atmospheric refraction. The receiving sites for the experiment employed low-noise preamplifiers and custom-made helical beam antennas as well as standard Air Force communications receiving equipment.

DD FORM 1 JAN 73 1473 EDITION OF 1 NOV 65 IS OBSOLETE

Unclassified

SECURITY CLASSIFICATION OF THIS PAGE (When Data Entered)

406820

ACKNOWLEDGMENTS

The authors would like to express their thanks for the assistance given by the 2054 Communications Squadron at Sheppard A.F.B., by the Air Force Weapons Laboratory, and by R & D Associates, Marina del Rey, CA.

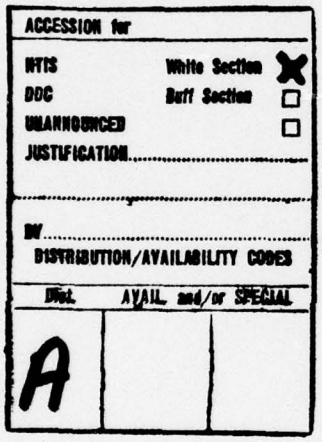

RESEARCH STAFF

Lubbock receiving site

J. D. Hill (Texas Tech Univ.)
T. L. Simpson (Texas Tech Univ.)
L. Bailin (R&D Associates)
F. Thibadeaux (Magnavox Corp.)

Sheppard A.F.B. receiving site

T. F. Trost (Texas Tech Univ.)
P. E. Garrison (Texas Tech Univ.)
G. Kahn (U.S.A.F.)
L. Martin (Magnavox Corp.)

TABLE OF CONTENTS

1. INTRODUCTION

This report summarizes the results of a UHF radio propagation experiment involving the transmission of AM voice signals between ground-based stations via a high-altitude transponder. The transponder was carried aloft by a N.A.S.A. Orion rocket to an altitude of 200 thousand feet and then parachuted back to earth. The parachute and the payload assembly containing the transponder were designed by N.A.S.A. and the transponder used a modified ARC-164 transceiver made by the Magnavox Corp. The experiment was organized by the Air Force.

The rocket was launched from the White Sands Missile Range, New Mexico, at 12:30:01 UT on July 14, 1977. A transmitter located about 60 miles from the launch site on Salinas Peak broadcasted prerecorded voice messages at a frequency of 241.5 MHz; these were re-transmitted by the transponder at 387.2 MHz to three receiving sites located at Lubbock, Texas, Sheppard Air Force Base, near Wichita Falls, Texas, and Peterson Field, near Colorado Springs, Colorado. Site locations are shown in Fig. 1-1.

As the parachute descended, it drifted slowly westward with the upper level winds. Signals were received from the transponder for a little over one half hour, after which time all of the receiving sites were below the radio horizon for the transponder. Here the term radio horizon means the horizon

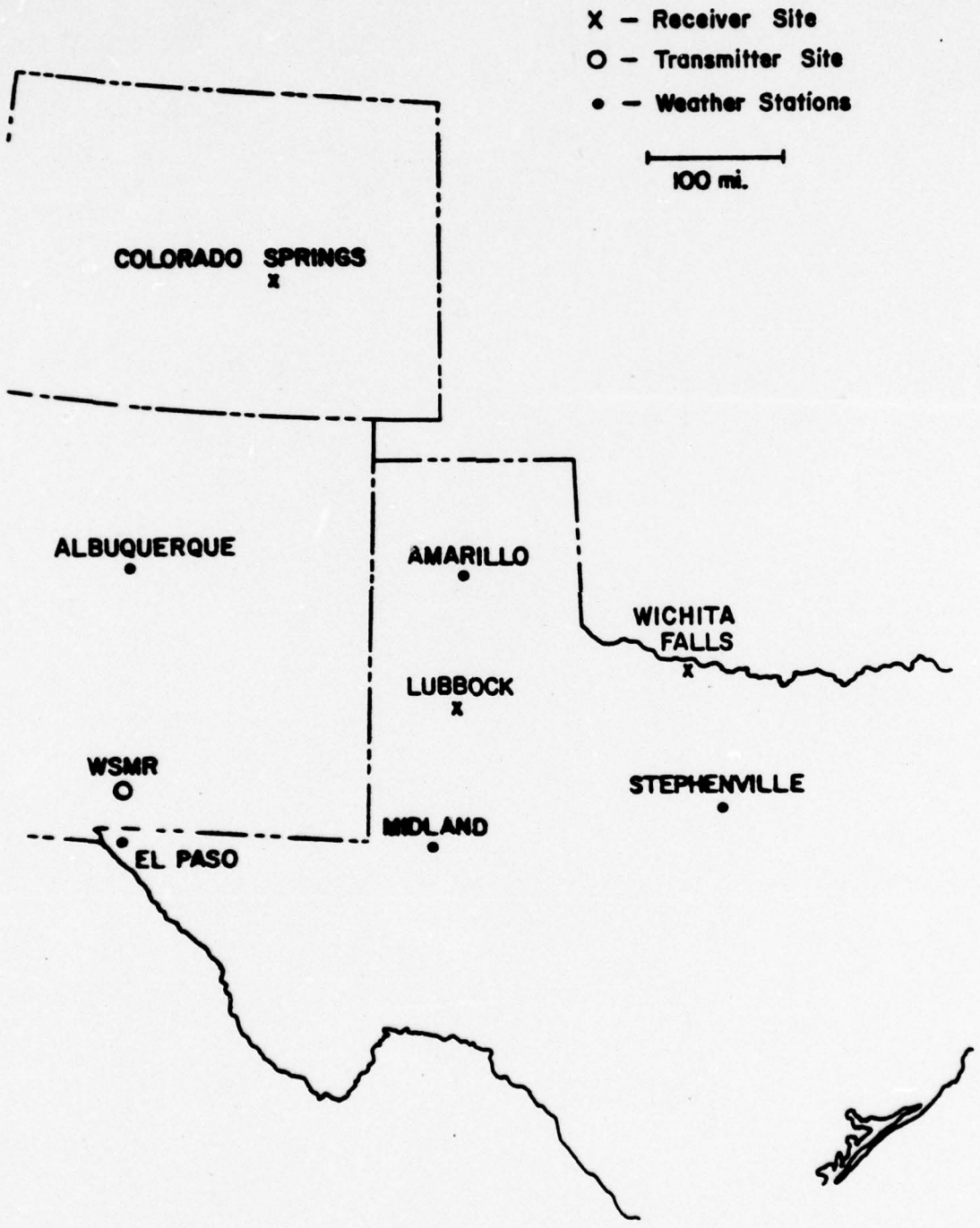

Fig. 1-1. Map of transmitting and receiving sites for the transponder flight. Stations supplying weather data also shown.

located by taking the radius of the earth to be 4/3 times its actual value. Using the larger radius allows for the refraction the waves undergo in the atmosphere, as explained in Chapter 5.

The Electrical Engineering Department at Texas Tech University assembled and operated the receiving sites at Lubbock and Sheppard A.F.B.; hence this report deals primarily with the data obtained at these sites. At both sites analog tape recordings were made of the voice messages and the carrier strength of the received signals. The recorded carrier-strength data were compared with a theoretical estimate based on the location of the payload as a function of time and an approximate knowledge of the atmospheric conditions during the flight. Signal variations present in the data which were not predicted by the calculations were also examined.

Chapter 2 of the report discusses the receiving systems at Lubbock and Sheppard, and Chapter 3 describes the design of our helical receiving antennas. Chapters 4 and 5 present the experimental results and the carrier-strength calculations, respectively.

One problem encountered during the flight was the loss of sufficient received signal strength at the transponder. This activated an auxiliary circuit in the transponder which caused the transmitter section to send an internally-generated 1020 Hz tone. The condition occurred intermittently, and as

a result the received voice messages were interrupted by tones. Additional discussion of this problem is given in Chapter 4.

2. RECEIVING SYSTEMS

To minimize the possibility of the loss of data due to an equipment failure, each receiving site used two complete receiving systems, consisting of an antenna, receiver, and tape recorder. At Sheppard A.F.B. system A employed a helical antenna built by us at Texas Tech, a low-noise preamplifier mounted at the antenna, and an ARC-164 receiver; system B used one of the standard Sheppard UHF communications receiving systems: an AS-1097 colinear dipole array antenna and a GRR-24 receiver. Table 2-1 compares the performance of the two systems. See Chapter 3 for details of the helical antenna design.

Because of the low-noise preamp and the higher gain antenna, system A had greater sensitivity than system B and received an intelligible signal for as long as the Sheppard receiving site remained above the radio horizon. System B was just barely able to detect the signal for a few seconds.

TABLE 2-1

Receiving Systems at Sheppard A.F.B.

Characteristic	System A	System B
Receiver sensitivity* (at antenna terminal)	-132	-113 dBm
Antenna gain (vert. polarization)	9	5 dBi

*For (S+N)/N = 3dB measured on HP 427A voltmeter (80% 1kHz modulation).

Both receiving systems were located at the Sheppard communications receiver site, with antennas (helix and AS-1097) atop standard 50 ft. antenna towers. A block diagram of system A is shown in Fig. 2-1. All the compments in Fig. 2-1 are identified in Table 2-2. Figure 2-2 is a photograph of the helix during assembly of the mounting brackets at Sheppard, and Fig. 2-3 shows the helix in position on the tower.

TABLE 2-2

Components Appearing in Figure 2-1

Label in Fig. 2-1	Component
A1,Q	Helical antenna with quarter-wave transformer
F	Bandpass filter (Spectrum Intl. Mod. PSF 387)
P	Preamplifier (Janel Mod. PCCM 7703)
S1,S2	Coaxial switches
B,J	12 V batteries and junction box to supply preamp power via coax
R1	ARC-164 receiver tuned to 387.2 MHz
SG	Signal generator (Wavetek Mod. 3000)
A2	Test dipole antenna
A3,R2	WWV monopole antenna and receiver (Drake Mod. DSR-2)
T1	Tape recorder (Sony Mod. TC-280)
T2	Tape recorder (Lockheed Mod. 417)
CR	Chart recorder (Houston Inst. Mod. 2-3000)

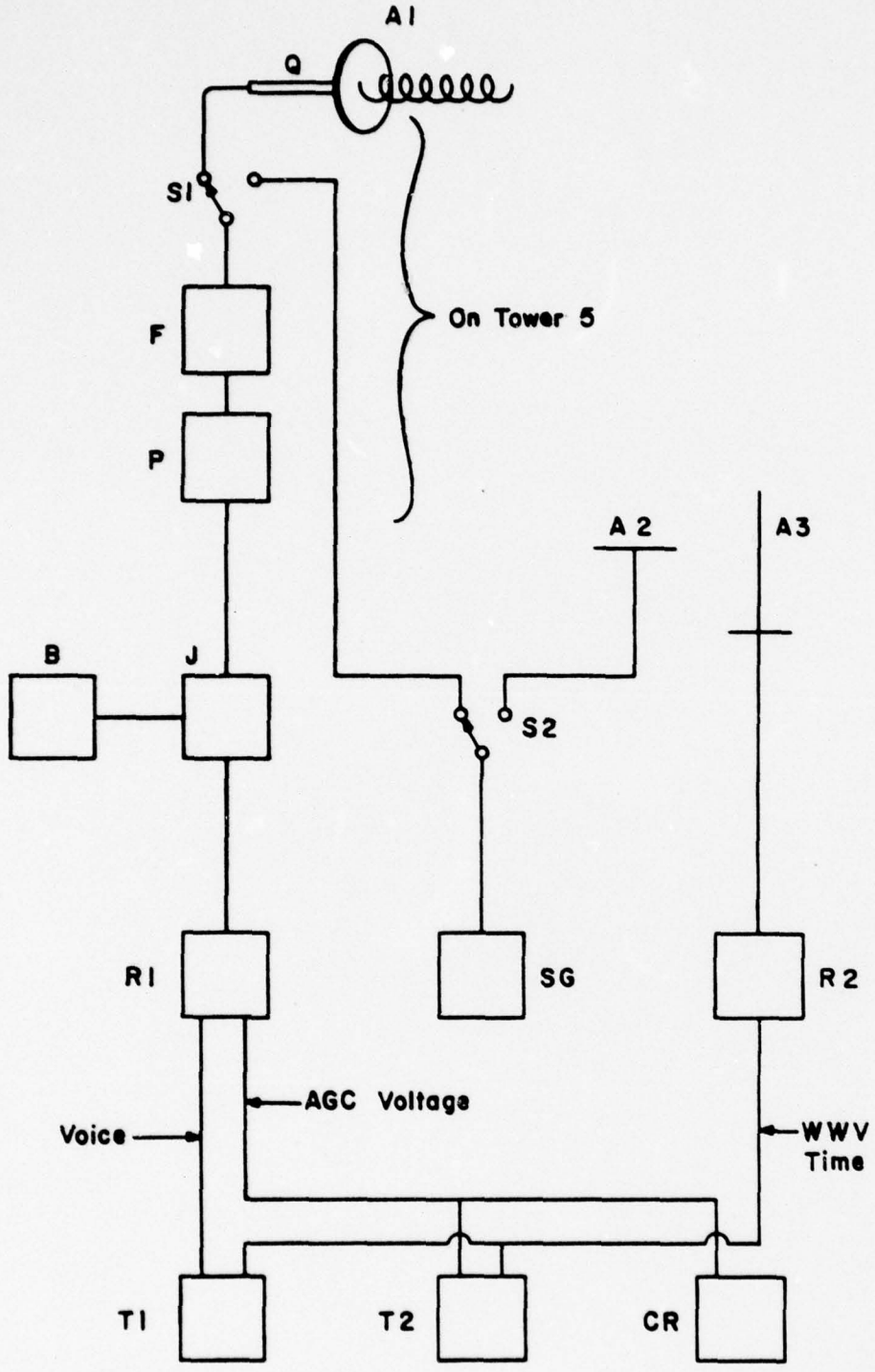

Figure 2-1. Block diagram of receiving system A at Sheppard A.F.B.

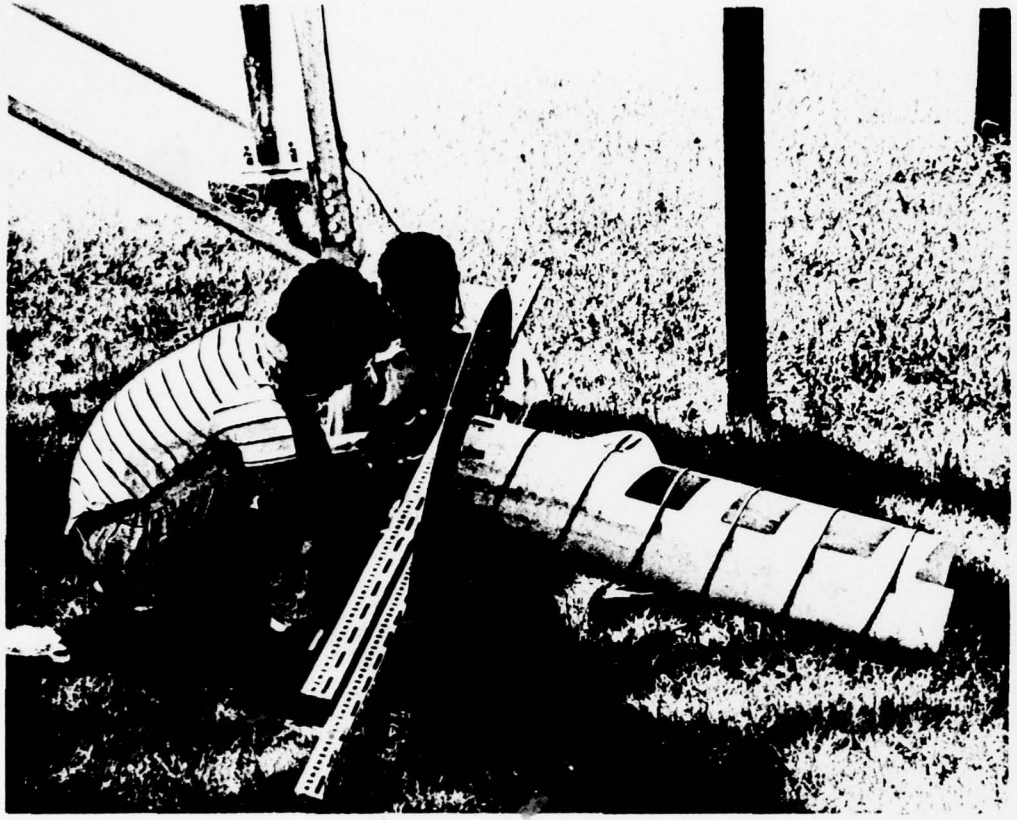

Figure 2-2. System A helical antenna.

Figure 2-3. System A helical antenna on tower at Sheppard A.F.B.

The basic components of System A were the antenna (A1), preamp and receiver (P,R1), and tape recorders (T1,T2). The system also had three embellishments. First, a high-quality signal generator, denoted SG, was included so that a known signal level could be introduced through switch S1 for receiver calibration or radiated from dipole A2 as an over-all system check. S1 and S2 were solenoid switches which were energized from a control panel along side the receiver. The panel was built by J. D. Hill. Second, an HF receiver, R2, was used to obtain accurate time information from radio station WWV at 5MHz. The time was recorded on the tape along with the voice and AGC voltage. Third, a chart recorder, CR, provided a visual display of the AGC voltage. Data on the carrier strength versus time from the AGC voltage is presented in Chapter 4 and compared with theory in Chapter 5.

The receiving systems employed at Lubbock were somewhat different than those at Sheppard. Lubbock system A used a helical antenna, preamp, and ARC-164 receiver just as at Sheppard, but System B used a double helix array antenna borrowed from New Mexico State University together with a second ARC-164 receiver. Due to a last-minute failure of System A, only system B received signals from the transponder. The gain of the system B antenna was measured to be 8 dBi and the sensitivity at the antenna terminals -121 dBm (for 3 dB (S+N)/N). The block diagram for System B is shown in Fig.

2-4, with components identified in Table 2-3. The double helix antenna was mounted on the roof of the Electrical Engineering Department's antenna site building, about 10 ft. above ground level. The receiving equipment for both the A and B systems was mounted, for convenience, in a single 6-ft. rack inside the building. See Fig. 2-5.

TABLE 2-3

Components Appearing in Fig. 2-3

Label in Fig. 2-3	Component
A1	Helix antenna array
S1,S2	Coaxial switches
R1	ARC-164 receiver tuned to 387.2 MHz
SG	Signal generator (Wavetek Mod. 3000)
A2	Test dipole antenna
A3,R2	WWV dipole antenna and receiver (Hammarlund Mod. SP-600)
T1	Tape recorder (H.P. Mod. 3960)
CR	Chart recorder (Sanborn Mod. 297)

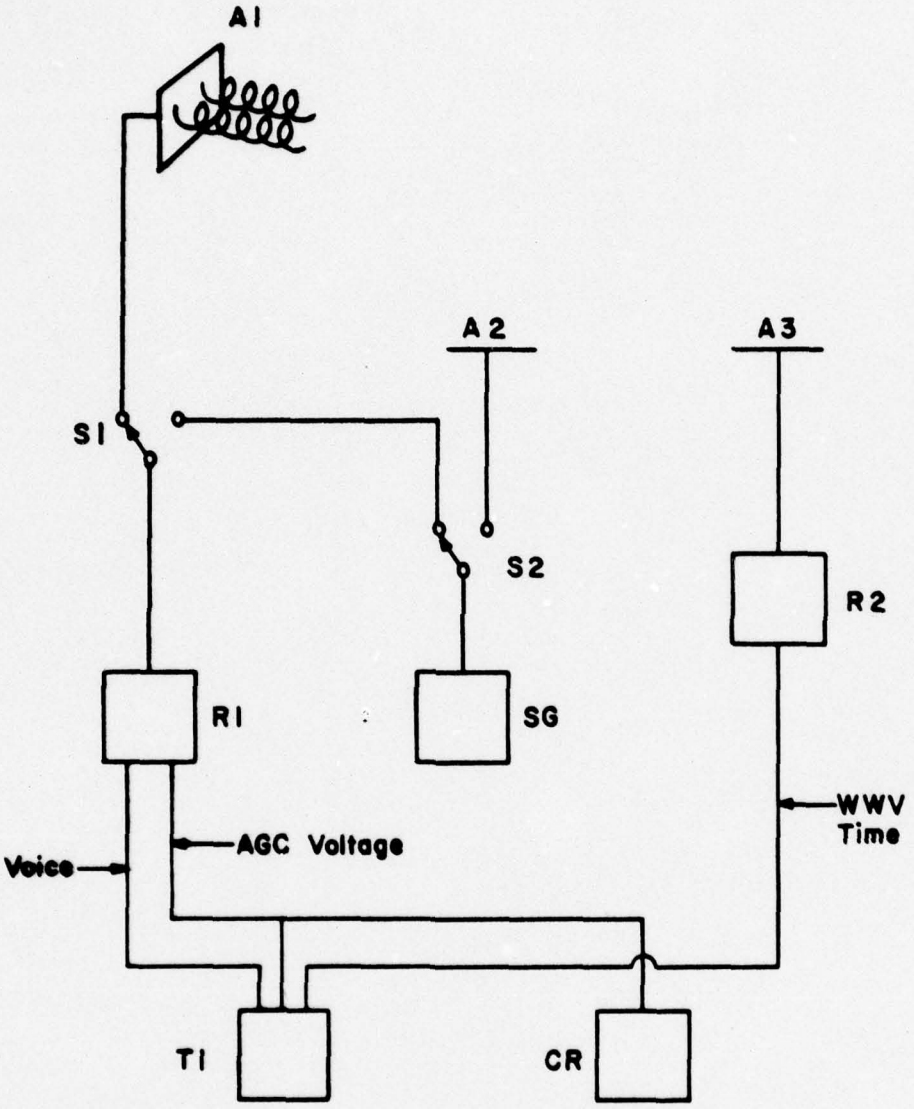

Figure 2-4. Block diagram of receiving system B at Lubbock.

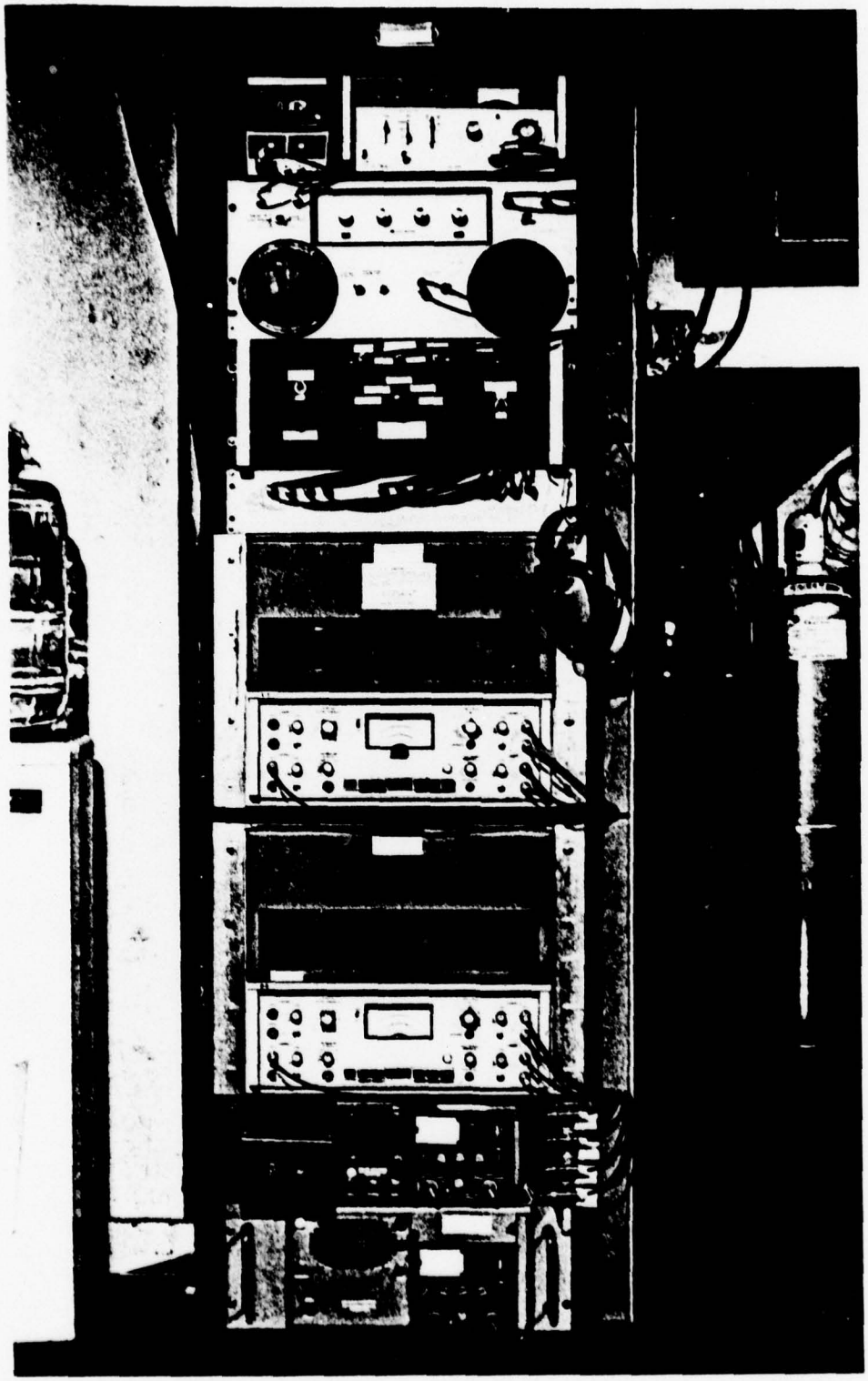

Figure 2-5. Receiving equipment at Texas Tech antenna site in Lubbock.

3. HELICAL ANTENNA DESIGN

Since the polarization of the signal at the receiving sites was a function of the orientation of the transponder, which varied somewhat, a receiving antenna whose gain was not a function of polarization was required to maintain a strong received signal. The helical beam antenna was a logical choice.

Figure 3-1 shows the relationship between circumference, C, spacing, S, turn length, L, and pitch angle, α, of a helix. D is the diameter of the helix measured from center to center. The approximate gain of a helical antenna is given by [1]:

$$G = 15\, C_\lambda n S_\lambda = 15 C_\lambda^3\, n \tan\alpha$$

where:

G = gain

C_λ = the circumference of the helix in free-space wavelengths

S_λ = the spacing between turns in free space wavelengths

n = the number of turns

α = the pitch angle

The circumference of the helix is not critical as the helix will operate in the axial mode, as desired, if C_λ is between 0.7 and 1.4 [2]. If the helix is wound around a 10-inch diameter form using 1/4-inch conductor, D is 10.25 inches and at 387.2 MHz C_λ is 1.06. For a helix of six turns and pitch angle of 13.5° the gain is given by:

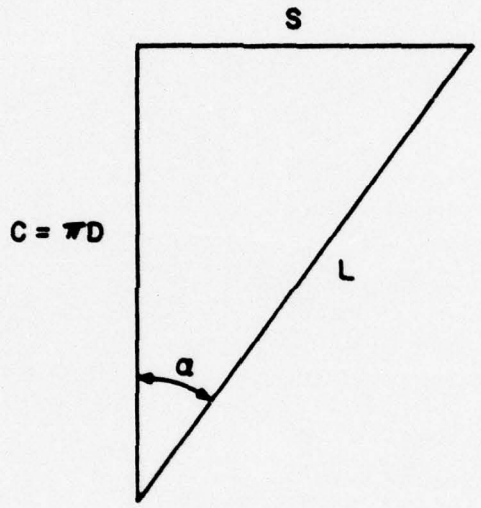

Figure 3-1. Relation between circumference, spacing, turn length, and pitch angle of a helix.

$$G = 15(1.06)^3(6)\tan 13.5°$$

$$= 25.42$$

$$10 \text{ Log } G = 14 \text{ dBi}$$

This is the theoretical gain of the helix when receiving a circularly polarized wave. If the received signal is linearly polarized, the gain is 3dB less or 11dBi.

The helix was constructed to the dimensions above by winding 1/4-inch copper tubing around a 10-inch plastic pipe at a pitch angle of 13.5°. The helix was also connected to a 32-inch circular ground plane. In this configuration the gain was 7.7 dBi. It was thought that the plastic pipe decreased the phase velocity of the wave on the helix resulting in slightly lower gain. To remedy this, the pitch angle was reduced to 11° producing a gain of 8.8 dBi, still a bit lower than the approximate theoretical value of 11 dBi. Large ports were also cut into the sides of the plastic pipe to reduce wind loading.

The terminal impedance of a helix operating in the axial mode is almost a pure resistance given by [3]:

$$R = 140\ C_\lambda\ \Omega$$

$$= 140\ (1.06)\Omega$$

$$= 148.4\ \Omega$$

To better match the helix to 50-ohm coaxial cable, a quarter-wave section of 75-ohm cable (RG-11) was connected to the helix terminal, producing a VSWR of 1.58.

The measured pattern of the helix is shown in Figure 3-2.

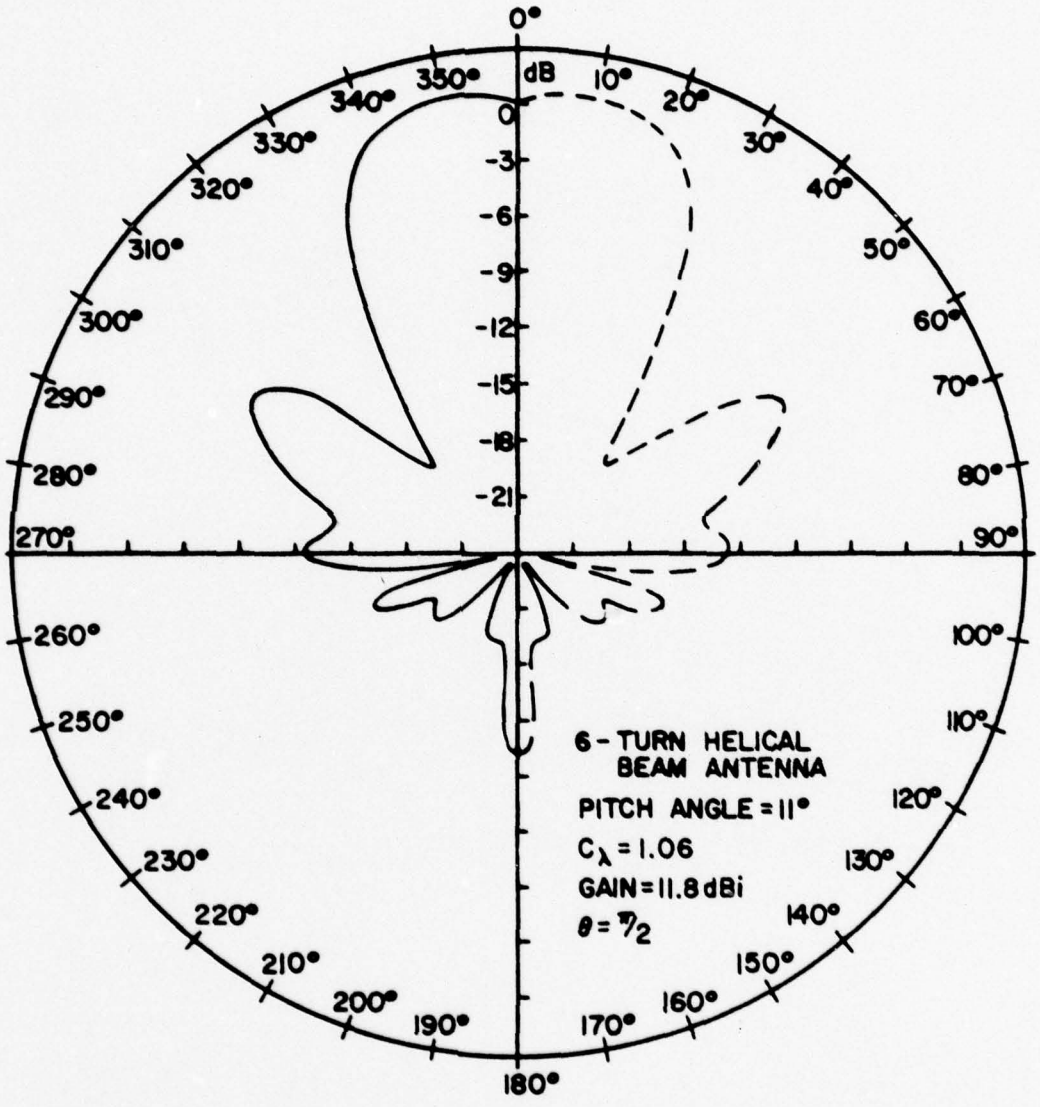

Figure 3-2. Antenna pattern for the 6-turn helix.

4. EXPERIMENTAL RESULTS

Signal Strengths

Signals of good quality were received from the transponder at all three receiving sites. Maximum signal levels were in the microvolt range, as expected on the basis of simple free-space propagation calculations. First detection of the signals at all the sites occurred during the first minute of the rocket flight, before separation of the rocket and payload (which occurred after 1 min 33 sec). Signal reception continued at Sheppard and Peterson for 8 min and at Lubbock for 34 min. The maximum in the carrier strength at Lubbock occurred from 6 to 11 minutes after launch (12:36 to 12:41 UT) with peaks at -98 dBm (3μV) and with valleys about 6 dB lower due to the payload roll, as discussed below. Carrier strength versus time for Sheppard is plotted in Fig. 5-8. The signal variations due to payload roll are the very closely spaced ones seen throughout the figure. There are in addition a few slower but stronger signal variations near the start and the end of the curve caused by propagation effects.

Signal Fading due to Payload Roll

One obvious characteristic of the signals was a quasi-periodic fading of the carrier strength with an average period of 5 sec and an average depth of 6 dB. The fades were found to occur at the same time at Lubbock and Sheppard. To determine the cause of the fading, telemetry data* from the payload were

*Telemetry and other data supplied by M. Sullivan, R&D Associates.

examined; and it was found that the fading was correlated with the payload roll (spin about vertical axis), with two fades per complete revolution of the payload. Thus, the fading evidently resulted from the variation in the radiation pattern of the transmitting antenna around the side of the payload as the payload rolled. Fading occurred simultaneously at Lubbock and Sheppard since these sites were located nearly along the same line of sight to the payload (Fig. 1-1). The transponder actually used an array of 4 antennas for transmitting, arranged ninety degrees apart around the side of the payload. The polarization of the transmitted signal was essentially along the axis of the payload, that is, vertical.

Figure 4-1 shows a comparison of the signal strength data from Lubbock and Sheppard and the payload roll magnetometer output given by the telemetry. Note the good correlation between the three curves.

Intermittent Tones

The voice messages were interrupted by unwanted tones, as mentioned in Chapter 1; and the tones were most frequent during the early part of the flight. The transponder was designed to send a tone only upon loss of the signal received from Salinas Peak. Apparently the received signal level really did drop; telemetry data from the payload shows a rough correlation between the AGC voltage of the transponder receiver and the

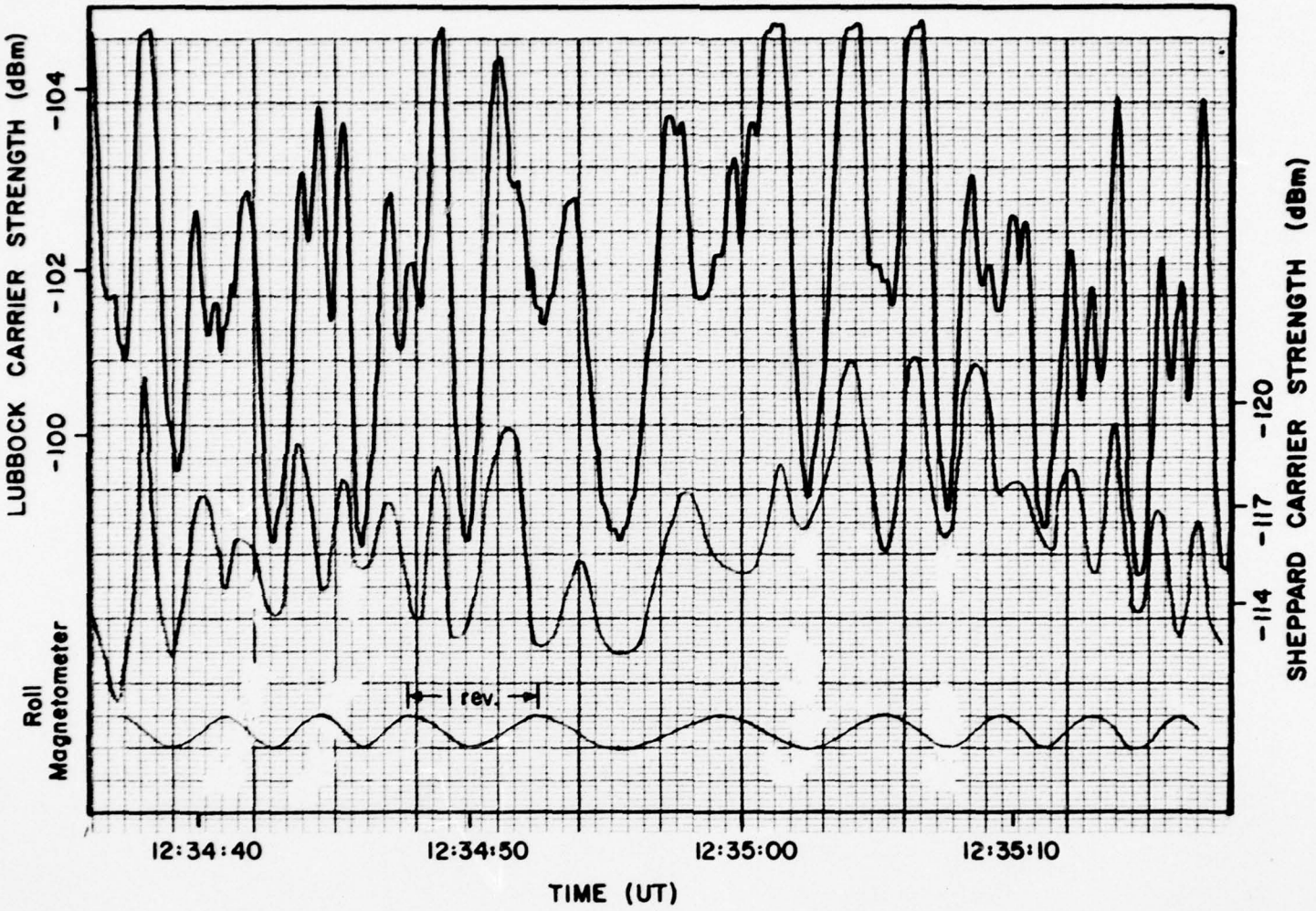

Figure 4-1. Comparison of received carrier strengths and payload roll.

occurrence of the tones. For some reason the correlation is not perfect, however. We now suggest how the signal loss might have happened by considering the following points:

1. The transponder used an array of two antennas located 180° apart on the payload for reception at 241 MHz. One of the antennas was found to be broken when the payload was recovered after the flight. It may have been broken throughout the time of the flight.
2. A comparison of the occurrence of the tones and the roll angle of the payload shows that early in the flight the tone came on once each revolution and remained on over a specific range of the roll angle.
3. The transmitting antenna (TACO AS-505A/GR) on Salinas Peak was a vertical array with a radiation pattern having a very flat main lobe. The antenna data sheet specifies a beamwidth of less than 20° with a slight tilt (5°) up from horizontal. The initial elevation angle of the payload from Salinas Peak was 30°, so during the early part of the flight the payload was high enough to be just above the main lobe. Thus the transponder received weak signals. Gradually the payload descended into the main lobe.
4. Thus we conclude it is likely that the combination of the broken receiving antenna and the weak signal from Salinas Peak caused the transponder receiver to experience such a weak signal that the tone was activated.

Figure 4-2 shows, for a short portion of the flight, the times when the tone was on, the AGC voltage of the transponder receiver, and the payload roll angle from the roll magnetometer. The tick marks on the roll angle curve give the times when the tone went on and off. The correlation between the three curves is clear.

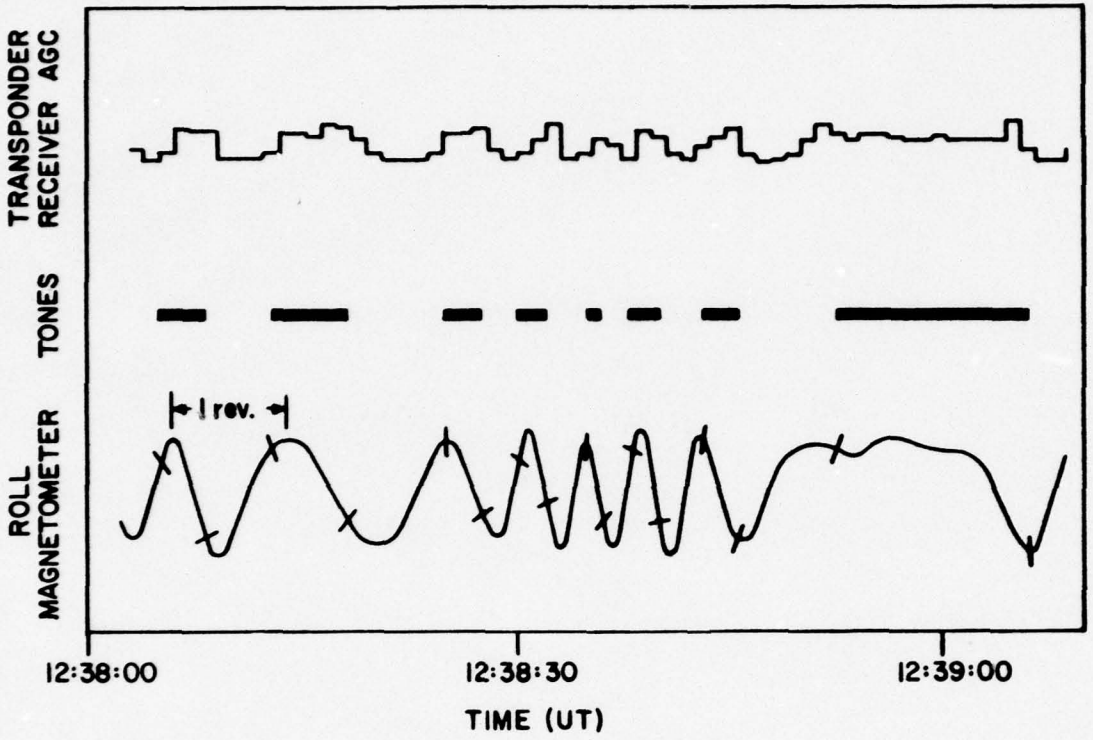

Figure 4-2. Comparison of transponder receiver AGC voltage, tone occurrence, and roll angle.

5. SIGNAL STRENGTH CALCULATIONS

The purpose of this chapter is to show how reflection, refraction, and diffraction effects were included in the calculation to estimate received signal strengths at Sheppard A.F.B. The first section outlines the calculations involved in obtaining the refractive modulus as a function of height. In the second section the 4/3 earth radius approximation is derived [4] and it is shown that this approximation is appropriate in light of the calculated refractive modulus profiles for the morning of the transponder flight. The third section outlines the steps involved in calculating the propagation factor which is then used to calculate received signal strengths [5]. Also included is a discussion of the effects of surface roughness on the calculated signal strength. The succeeding sections present details of the calculations and interpretation of the results.

Calculation of Refractive Modulus and Dynamic Height

Since the refractive index of the atmosphere is very nearly unity, it is more convenient to think in terms of the refractive modulus which is defined as

$$N = (n-1) \times 10^6$$

where n is the refractive index. The refractive modulus of the atmosphere can be determined from the temperature, pressure, and dew point temperature [6].

$$N = \frac{79P}{T} - \frac{11e}{T} + \frac{3.8\times10^{5}\, e}{T^{2}} \quad ,$$

where

P = barometric pressure in millibars

T = temperature in degrees K

e = water vapor pressure in millibars

The barometric pressure and temperature are obtained from National Weather Service radiosonde data. The saturation vapor pressure at the dew point temperature is the partial pressure of water vapor. By using temperature versus saturation vapor pressure tables [7] and dew point temperatures from the radiosonde data, the water vapor pressure, e, can also be determined.

The refractive modulus is usually plotted versus altitude or "dynamic height." To determine the dynamic height, consider the forces on the differential volume shown in Fig. 5-1.

$$\begin{aligned} A\, dp &= -A\rho g dh \\ dp &= -\rho g dh \end{aligned} \qquad (1)$$

which says that the differential pressure, dp, is related to the mass density, ρ, the acceleration due to gravity, -g, and a differential element of height dh. From the ideal gas law

$$n = \frac{P}{kT} \quad , \qquad (2)$$

Figure 5-1. Differential volume for calculating dynamic height.

where n is the particle density, p is the pressure, k is Boltzmann's constant and T is temperature in degrees K. Multiplying equation (2) by the average mass of air per particle, m, gives

$$nm = \rho = \frac{mp}{kT} \qquad (3)$$

substituting (3) into (1) gives

$$dp = -\frac{mpg}{kT}\,dh$$

$$\frac{T}{p}dp = -\frac{mg}{k}\,dh$$

$$\int_{p_1}^{p_2} \frac{T}{p}dp = -\int_{h_1}^{h_2} \frac{mg}{k}\,dh = \frac{mg}{k}\,(h_1-h_2)$$

Using numerical integration, h_2 can be determined if T, P, P_1, P_2 and h_1 are known. The NWS radiosonde data provides temperature versus pressure information, so that if the height above sea level of the ground level is known, a dynamic height for each temperature and pressure may be calculated. Since each temperature and pressure also determines the refractive index, the refractive modulus may be plotted versus dynamic height. The calculated refractive modulus profiles for Albuquerque, New Mexico, Amarillo, Texas, El Paso, Texas, Midland, Texas, and Stephenville, Texas using the 12Z radiosondes on 14 July 1977 are shown in Fig. 5-2.

The 4/3 Earth Radius Approximation

For the case when the refractive index is assumed to vary only with height, as shown in Fig. 5-3, Snell's Law of refraction becomes:

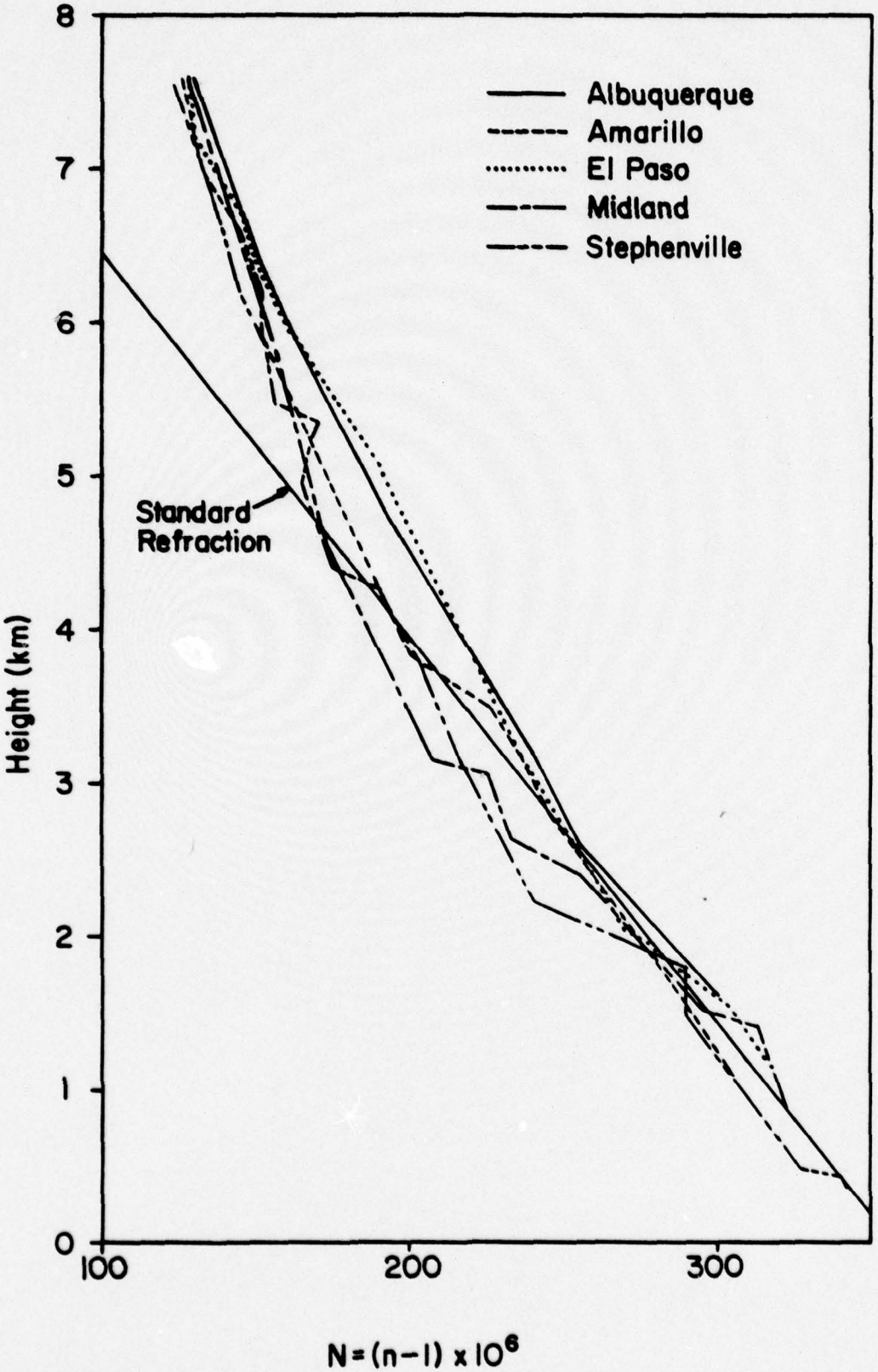

Figure 5-2. Refractive modulus profiles calculated from 12 Z radiosondes on July 14, 1977.

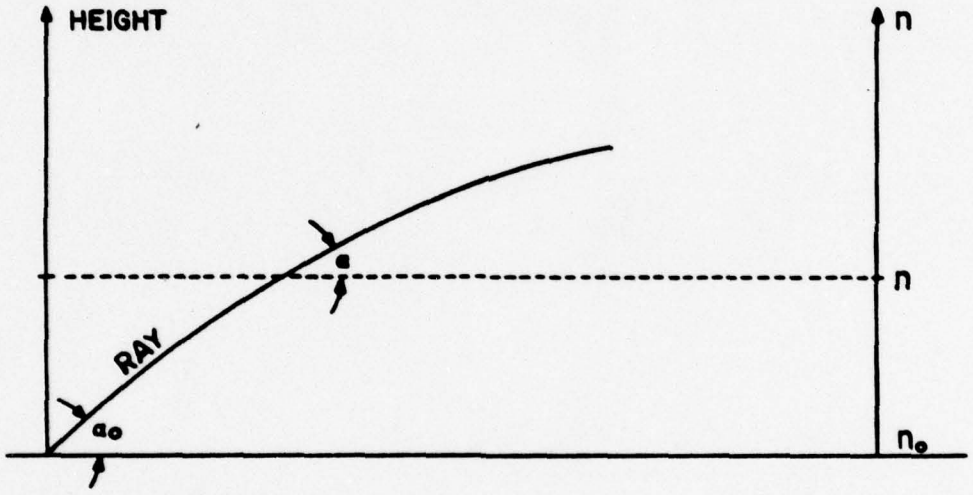

Figure 5-3. Snell's Law of Refraction for a continuously varying index.

$$n \cos\alpha = n_o \cos\alpha_o$$

To determine the amount of bending of a ray in the atmosphere, consider Fig. 5-4. BC represents a wave moving in the direction of CE. After a time dt, B and C move to points D and E respectively. The index at C is n and at B is n+dn. In Fig. 5-5, ρ is the radius of curvature of the path CE. Also,

$$nv = c$$

where n is the index of refraction, v is the velocity of the wave, and c is the speed of light. If the velocity at C is v and the velocity at B is v+dv, then

$$nv = (n+dn)(v+dv)$$

$$nv = nv + ndv + vdn + dvdn$$

Assuming that the second order term is negligible and solving for v gives:

$$v = -n \frac{dv}{dn} \qquad (4)$$

The length of the rays CE and BD are s and s+ds respectively.

$$s \equiv vdt \qquad (5)$$

$$s+ds = (v+dv)dt$$

$$ds = dvdt \qquad (6)$$

From Fig. 5-4

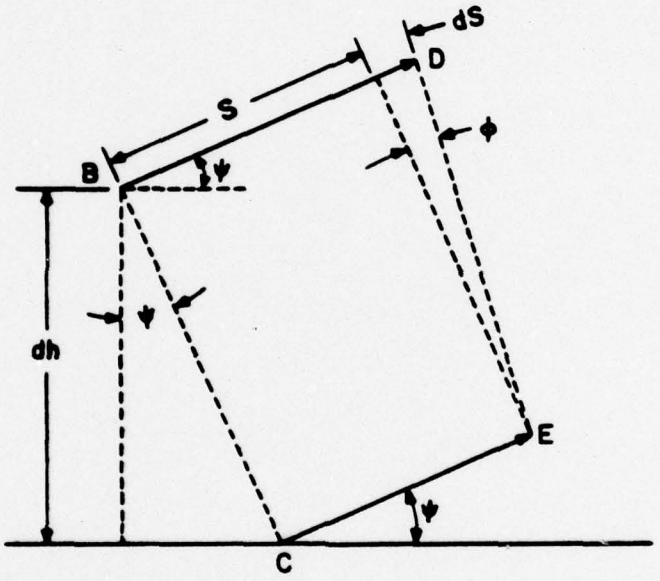

Figure 5-4. Geometry to determine ray bending

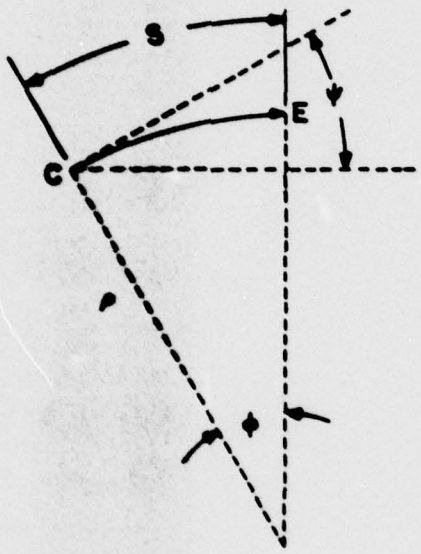

Figure 5-5. Earth geometry for curve CE

$$\cos\psi = \frac{dh}{BC}$$

$$\tan\phi = \frac{ds}{BC} = \frac{ds}{dh}\frac{dh}{BC}$$

$$\tan\phi = \frac{ds\ \cos\psi}{dh}$$

$$\tan\phi \simeq \phi = \frac{ds\ \cos\psi}{dh} \qquad (7)$$

since for small ϕ, $\tan\phi \simeq \phi$. From Fig. 5-5:

$$s/\rho = \phi \qquad (8)$$

substituting equations (4), (5), (6), and (8) into (7) gives:

$$\frac{dvdt\ \cos\psi}{dh} = \frac{-ndvdt}{\rho dn}$$

solving for ρ gives:

$$\rho = \frac{-n}{\frac{dn}{dh}\cos\psi}$$

Since ψ is a very small angle, $\cos\psi \simeq 1$, and since $n \simeq 1$

$$-\frac{1}{\rho} = \frac{dn}{dh} \qquad (9)$$

This means that the radius of curvature of a ray is equal to the negative gradient of the index of refraction, assuming that the index varies only with altitude. In general the index varies nonlinearly with height. However, in the lower atmosphere, $\frac{dn}{dh}$ is approximately constant, that is, a plot of n(or N) versus altitude is approximately linear.

If the radius of the earth is corrected, and it is assumed that the gradient of the refractive index is constant, rays

from a source in the atmosphere will be straight lines. To correct the radius of curvature of the earth let:

$$\frac{1}{a} - \frac{1}{\rho} = \frac{1}{ka} \qquad (10)$$

where a is the radius of the earth, ρ is the radius of curvature of a ray (nearly horizontal), and k is a constant. Substituting (9) into (10) gives:

$$\frac{1}{a} + \frac{dn}{dh} = \frac{1}{ka}$$

and solving for k gives:

$$k = \frac{1}{1+a\frac{dn}{dh}}$$

In the lower atmosphere $\frac{dn}{dh}$ is often approximately -3.9×10^{-5} n units per kilometer. The mean radius of the earth is 6.37×10^{3} kilometers so that:

$$k = 1.331 \simeq \frac{4}{3}$$

From the refractive modulus profiles, shown in Fig. 5-2, it can be seen that the curves are approximately exponential. However, below a height of around 4.5 kilometers the curves are approximately linear with an average slope of around -40 N units per kilometer. Therefore we are reasonably justified in making the 4/3 earth radius approximation in order to determine approximate signal strengths and lengths of time strong signals are received.

Calculation of Propagation Factor and Received Signal Strength

In free space, the ratio of received power to transmitted power is given by:

$$\frac{P_r}{P_t} = \frac{G_t G_r \lambda^2}{(4\pi R)^2} \left| f_t(\theta,\phi) f_r(\theta',\phi') \right|^2$$

where

P_r = received power

P_t = transmitted power

G_t = gain of transmitting antenna over isotropic source

G_r = gain of receiving antenna over isotropic source

λ = wavelength in free space

R = distance separating receiving and transmitting antennas

$f_t(\theta,\phi)$ = antenna pattern function of transmitting antenna

$f_r(\theta',\phi')$ = antenna pattern function of receiving antenna

The antenna pattern functions are defined such that their maximum value is 1.

The propagation factor, F, is defined as the ratio of the amplitude of the electric field at a given point under specified conditions to the amplitude of the electric field under free-space conditions with the beam of the transmitter directed toward the point in question:

$$F = \left| \frac{E}{E_o} \right|$$

In free space $F = |f_t(\theta,\phi)|$. However, in the presence of the earth F involves interference, diffraction, and refraction effects. For a smooth flat earth with no atmosphere the electric field

is given by the sum of the direct and reflected fields

$$E = E_d + E_r = E_o \left[f_t(\theta_1) + \rho f_t(\theta_2) e^{-j(\phi + k\Delta R)} \right]$$

where

E_o = free space electric field

E_r = reflected electric field

E_d = direct electric field

θ_1 = angle between antenna maximum and direct ray

θ_2 = angle between antenna maximum and reflected ray

ρ = magnitude of the reflection coefficient

ϕ = phase of the reflection coefficient

$k\Delta R$ = phase difference due to the path length difference between direct and reflected rays

If the 4/3 earth radius spherical earth is used to model atmospheric refraction, a divergence factor, D, must be included to account for the divergence of rays reflected from a spherical surface. D is included in the following way:

$$F = \left| f_t(\theta_1) + D\rho f_t(\theta_2) e^{-j(\phi + k\Delta R)} \right|$$

Since the transponder was spinning, it is more convenient to give the transmitting antenna an average gain independent of θ and ϕ, in which case F becomes:

$$F = \left| 1 + D\rho e^{-j(k\Delta R + \phi)} \right|$$

The geometry of the transmitter-receiver system is shown in figure 5-6. To more easily determine ΔR, D, and ψ_2 it is necessary to introduce the dimensionless parameters S and T

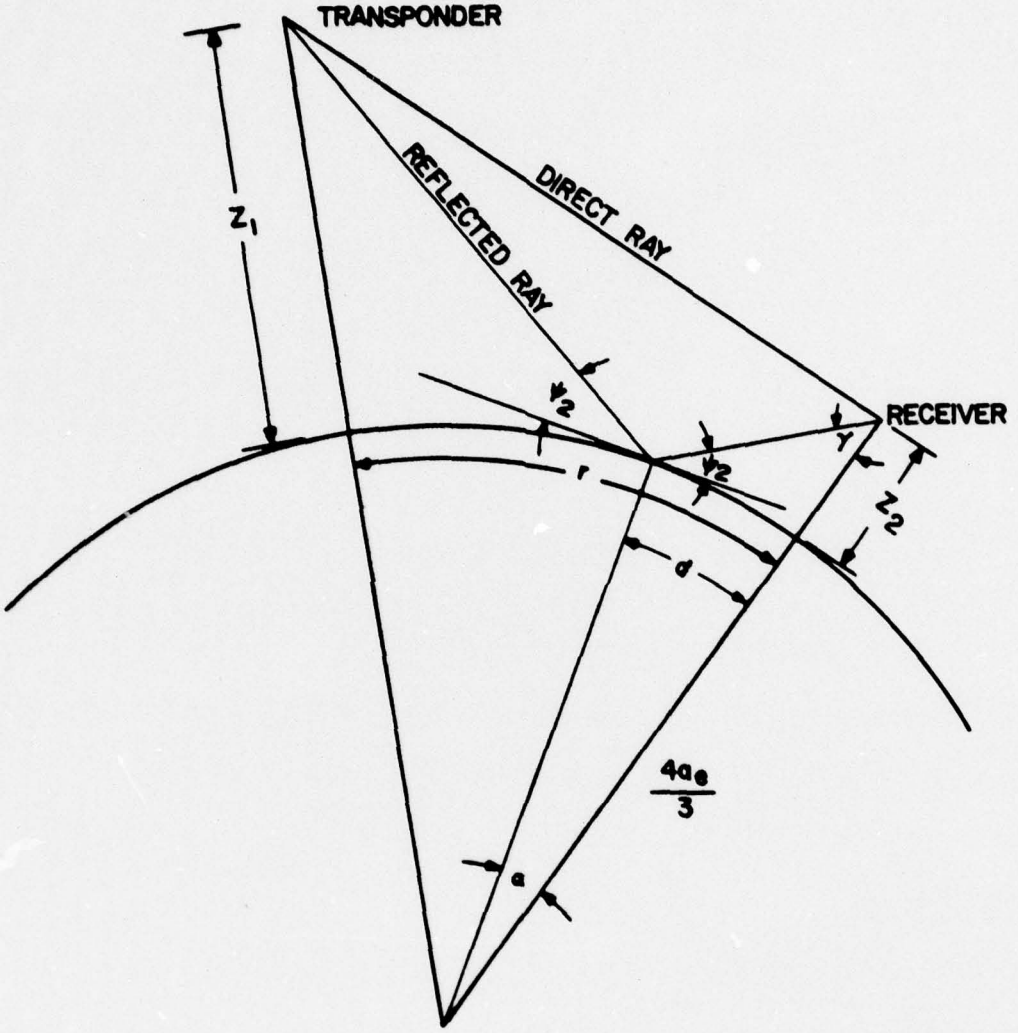

Figure 5-6. Geometry of transponder and receiver system, showing the grazing angle ψ_2, the height of the transponder Z_1 and the height of the receiving antenna Z_2.

given by:

$$S = \frac{r}{\sqrt{2r_e z_1} \quad \sqrt{2r_e z_2}}$$

$$T = \sqrt{\frac{z_2}{z_1}}$$

where r is the distance, measured in miles along the earth, between the transmitter and receiver, and for the 4/3 earth radius model, r_e is 5280 miles. z_1 and z_2 are measured in feet and represent the height of the transponder and receiving antenna respectively.

$$\tan\psi_2 = \frac{z_1+z_2}{r} \quad K(S,T)$$

$$D = D(S,T)$$

$$\Delta R = \frac{2z_1 z_2}{r} J(S,T)$$

If s and T are known, J(S,T), K(S,T) and D(S,T) can be determined graphically.

The reflection coefficient Γ for a vertically polarized wave is given by [8]:

$$\Gamma = \rho e^{-j\phi} = \frac{(\frac{k_1}{k_o})^2 \sin\psi_2 - \sqrt{(\frac{k_o}{k_1})^2 - \cos^2\psi_2}}{(\frac{k_1}{k_o})^2 \sin\psi_2 + \sqrt{(\frac{k_o}{k_1})^2 - \cos^2\psi_2}},$$

where:

$$(\frac{k_1}{k_o})^2 = \frac{\varepsilon}{\varepsilon_o} - j\,\frac{\sigma}{w\varepsilon_o}$$

The procedure for calculating F for the receiver site at Sheppard A.F.B. is summarized as follows:

1. Determine z_1 and r.
2. Calculate S and T.
3. Determine J(S,T), K(S,T) and D(S,T) graphically.
4. Calculate ΔR and ψ_2.
5. Calculate ρ and ϕ.
6. Calculate F.

The received signal strength is given by

$$P_r = P_t \frac{G_t G_r \lambda^2}{(4\pi R)^2} F^2 \mid f_r(\theta', \phi') \mid^2$$

Since the transponder was so far away from the receiving antenna, the gain of the receiving antenna was fairly constant, so that

$|f_r(\theta', \phi')|$ is approximately 1.

Three regions are defined with respect to the total radio horizon: the interference region, the intermediate region, and the diffraction region. These are shown in Fig. 5-7. It should be noted that the calculation summarized above is valid only when the receiving antenna is in the interference region, or symbolically when

$$S < 1$$

To determine signal strength in the intermediate region, F at the quadrature point ($\Delta R = \frac{\lambda}{4}$) is calculated along with F at a point sufficiently far into the diffraction region. Then

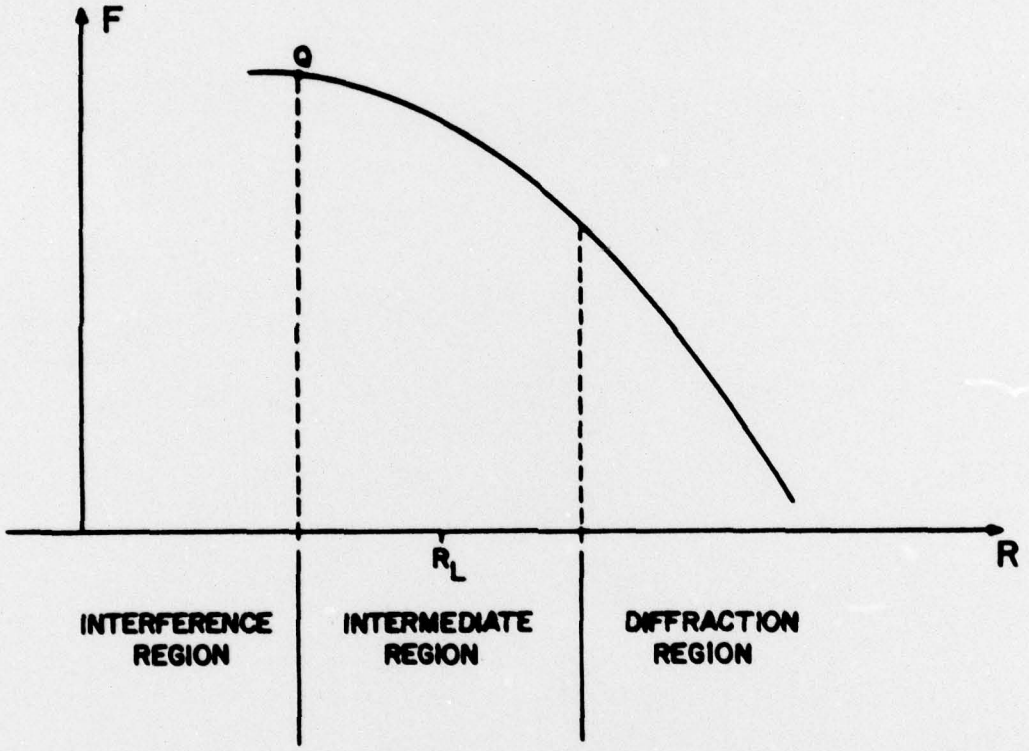

Figure 5-7. Plot of F vs. R showing interference, intermediate, and diffraction regions. Q is the quadrature point and R_L is the total radio horizon.

on a plot of F versus r, a straight line is drawn between these two points to show how F decreases in the intermediate region. However, since the transmitted power from the transponder was only 1 watt, the signal was strong enough to vary the receiver AGC only part way into the intermediate region. Therefore, because the signal strength data in this region was incomplete, calculation of the signal strength in the diffraction region was not justified.

To determine whether to expect diffuse or specular reflections from the earth, it is necessary to determine the area, smoothness, and location of the reflection point.

The reflection point can be thought of as a family of Fresnel zones, elliptical in shape. The approximate area of the Fresnel zones is given in the following way [9]:

$$A_n \simeq \frac{\pi r \sqrt{n\lambda r}}{4} \frac{1 + \frac{2\delta_o}{n\lambda}}{\left[1 + \frac{(z_1+z_2)2}{n\lambda r}\right]^{3/2}}$$

The approximate path length difference between the direct ray and any ray reflected from the first Fresnel zone is given by:

$$\delta_o = \frac{2z_1z_2}{r}$$

For the first, and most significant, Fresnel zone:

$$n=1$$

The other parameters are as previously defined. These approximations are valid as long as z_1, z_2, and δ_o are all much smaller than r.

For the surface to be considered smooth, the variation in height within the first Fresnel zone must satisfy the following condition [10]:

$$h < \frac{\lambda}{8 \sin\psi_2}$$

It is also of interest to determine the location of the center of the first Fresnel zone in order to determine if the smoothness condition is met by the terrain there. The location of the center of the Fresnel zone can be estimated using Fig. 5-6. From the law of sines:

$$\frac{\frac{4a_e}{3} + z_2}{\sin(90°+\psi_2)} = \frac{\frac{4a_e}{3}}{\sin\gamma}$$

$$\alpha = 90° - \psi_2 - \gamma$$

$$\gamma = \sin^{-1}\left[\frac{\frac{4a_e}{3}\sin(90° + \psi_2)}{R_E + z_2}\right.$$

$$d = \frac{\alpha}{360°} 2\pi \frac{4a_e}{3}$$

where d is the distance from the reflection point to the receiving antenna.

Details of the Calculations

To calculate the refractive modulus, the barometric pressure and temperature were obtained directly from National Weather Service radiosonde data. To find the water vapor pressure, the dew point temperature, which was also obtained from

the radiosonde data, was substituted for the temperature in the saturation vapor pressure tables, and the vapor pressure was read directly.

To calculate the dynamic height recall:

$$\int_{P_1}^{P_2} \frac{T}{P}\, dP = -\frac{mg}{k}\,(h_2-h_1)$$

Using the trapezoidal rule, and solving for h_2 gives:

$$h_2 = \frac{T_2}{2P_2} + \frac{T_1}{2P_1}\,(P_2 - P_1)\frac{k}{mg} - h_1$$

where

$k = 1.380 \times 10^{-23}$ J/K

$m = 4.809 \times 10^{-26}$ kgm.

$g = 9.80665$ m/sec^2

To calculate the first height, the temperature, pressure, and height above sea level of the surface is substituted in for T_1, P_1, and h_1, respectively. Also, the next temperature and pressure is substituted in for T_2 and P_2. To calculate the next height the preceding calculated value of h_2 is substituted for h_1, and T_2 and P_2 of the preceeding calculation become T_1 and P_1, respectively. The next temperature and pressure are substituted for T_2 and P_2. This procedure is repeated until all dynamic heights are calculated.

White Sands telemetry provided payload height and range data for the calculation of the propagation factor. Since the receiving antenna was above the radio horizon when the transponder was above approximately 105000 feet, propagation

factors were calculated for the range of heights from 105015 to 197015 feet above mean sea level, or 10400 to 196000 feet above Sheppard AFB. The transponder was within this range from 45.146 to 559.28 seconds after launch. During this time the range, r, varied from 466.8 to 477.0 miles. The height of the receiving antenna was constant at 50 feet. To calculate values for S and T, z was varied from 104000 to 196000 feet in increments of 4000 ft., z_1 was 50 feet, and r was determined from telemetry. J(S,T), K(S,T) and D(S,T) were determined graphically, and then, ΔR, ψ_2 and D were calculated. To calculate the reflection coefficient it was necessary to find a value for $(\frac{k_1}{k_o})^2$. The number 5.0-j.0.0465 for built up urban districts [11] was selected because of the proximity of the receiver site to Wichita Falls, Texas. With ρ, ϕ, ΔR and D, F were calculated along with P_r, the received signal strength. The average gain of the transmitting antenna was -4.5dBi, and the gain of the receiving antenna was 8.8dBi.

With Z_1, Z_2, r, and ψ_2, A, d, and h_{max} were calculated. h_{max} is the maximum height in the first Fresnel zone for the surface to be considered smooth, and is defined as follows:

$$h_{max} = \frac{\lambda}{8 \sin \psi_2}$$

Interpretation of the Results

A plot of the calculated received signal strengths at Sheppard AFB as a function of time is shown superimposed on the measured data in Fig. 5-8.

As the transponder descended from 197015 to 145015 ft, h_{max} increased from 8.7 to 23.8 ft., and then as the transponder descended below 145015 ft., h_{max} increased rapidly. This means that while the transponder was high, the surface at the reflection point should have behaved as a rough surface, producing diffuse reflections; and as the transponder descended, the surface should have behaved more and more as a smooth surface, producing specular reflections. As can be seen in Fig. 5-8, when the transponder was high, the signal was relatively constant indicating diffuse reflection, and the large variations when the transponder was low indicate specular reflections. It is also possible the signal variations occurred because either the reflected rays or both the direct and reflected rays were partially blocked at times by buildings or hills in the vicinity of the receiver site. There is also a possibility that at times there was more than one reflection point.

Since no points were calculated for the diffraction region, the plot of signal strengths before and after the quadrature points, shown by dashed lines in Fig. 5-8, are only estimates of the variation of signal strength in the intermediate region. Using these estimates, it can be determined that a signal strength of approximately -122dBm will

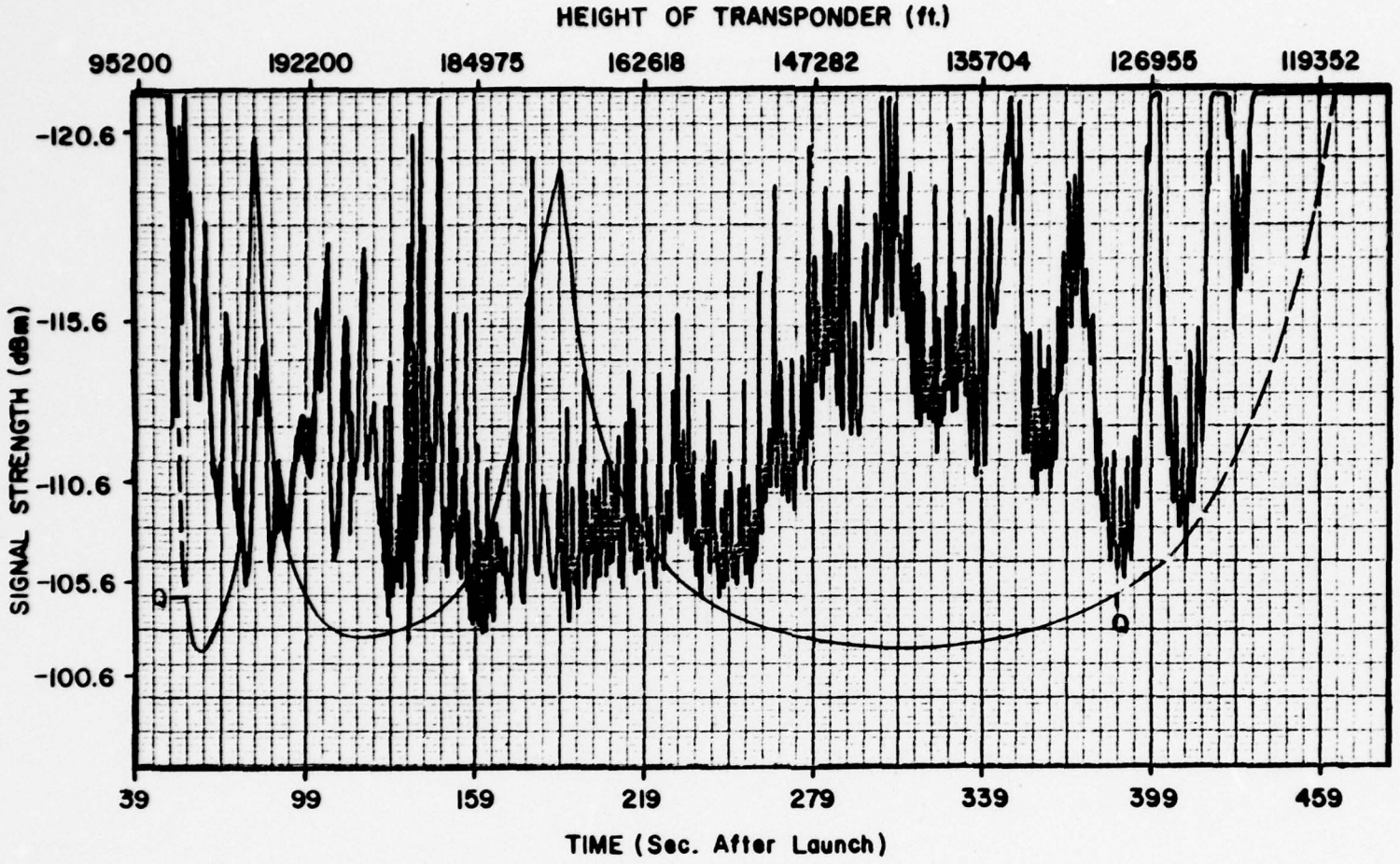

Fig. 5-8. Plot of received signal strength for Sheppard AFB as a function of time. Smooth curve represents calculated signal strength.

be reached at 52 sec. and again at 467 sec. after launch. These are the approximate points where the AGC should start and stop varying respectively. The actual measurements indicate that the AGC started varying at 51 sec. and stopped at 437 sec. after launch.

Since the signal strength decreases rapidly in the intermediate region, readable signals should be expected to continue for only a short time after the AGC becomes constant. The signal was heard up to 3 min. after the AGC became constant but readable transmissions ceased approximately 1 min. earlier.

As can be seen in Fig. 5-8, the maximum calculated signal strength is within 2dB of the measured maximum.

6. CONCLUSIONS

From a radio propagation standpoint, the transponder flight provided an interesting experiment because the rapid ascent and descent of the transmitting source allowed a continuous measurement of received signal strength from below the radio horizon to several degrees above and then back down again. The ascending and descending portions of the flight each resulted in a series of variations in the received signal, an interference pattern characteristic of the reflecting region of the terrain in front of the receiving antenna. This pattern is shown for the Sheppard receiving site by Fig. 5-8. The variations near the beginning of the measured signal strength curve occurred during the transponder ascent, and then a near duplicate of the variations, but proceeding in reverse order and more slowly, occurred during the descent near the end of the curve.

Because only a short period of time elapsed during the measurement in Fig. 5-8, the signal variations observed could not have been due to changes in atmospheric conditions along the signal path. Atmospheric effects of course could be very important over longer time periods.

The calculated curve of signal strength in Fig. 5-8 approximates well the start and end times and the maximum value of the measured curve, and it contains variations with some similarity to those of the measured curve. However, the calculated curve lacks the strong variations which occurred around the times of the quadrature points. Of course, the

calculations assume that the earth is perfectly smooth and of constant elevation over the reflecting region, and this was not the case. It would seem that one should be able to predict these variations with a good model of the terrain around Sheppard and ray tracing calculations applied to the reflecting region as it moved with time.

As described in Chapter 5, an analysis of the 12Z meteorological data from several locations in Texas and New Mexico on the day of the flight showed a refractive index variation with height not far from the "standard" value of -40 N units per kilometer. This variation is characteristic of a well-mixed troposphere. An examination of average 12Z N profiles for the month of July for the last three years also reveals a near-standard variation. Thus we know that the experiment was done under standard conditions and conditions which obtain on the average on July mornings over this part of the country.

Since the signal from the transponder was only barely detected at Sheppard with the standard Air Force receiving gear of System B, a natural question, and one posed by M. Sullivan, is what increase in the output power of the transponder would have been needed to obtain good reception with the standard Air Force equipment? The signal was detected on System B only when it reached its highest value, between 12:32 and 12:33 UT, and the level at this time was close to

the noise level of the system. During much of the time the signal level recorded by System A (Fig. 5-8) was within about 7 dB of the highest value, so an increase in transponder power of 7 dB would have made most of the signal rather than just the peak signal detectable on System B. This assumes the variations in the System B signal with time would have been like those of System A, which is a good assumption since the receiving antennas of the two systems were situated close to each other. In order to achieve a good signal-to-noise ratio, an additional increase of about 10 dB would have been needed. Thus the total power increase for good reception is 17 dB, or an increase in the transponder output from 1W to 50W.

REFERENCES

1. John D. Kraus, Antennas, (New York: McGraw-Hill Book Company, 1950), p. 213.

2. Ibid., p. 176.

3. Ibid., p. 213.

4. Henry R. Reed and Carl M. Russell, Ultra High Frequency Propagation, (Cambridge: Boston Technical Publishers, Inc., 1966) pp. 43-45.

5. Donald E. Kerr, Propagation of Short Radio Waves, Massachusetts Institute of Technology Radiation Laboratory Series, no. 13 (New York: McGraw-Hill Book Company, 1951), pp. 27-180.

6. Henry R. Reed and Carl M. Russell, Ultra High Frequency Propagation, (Cambridge: Boston Technical Publishers, Inc., 1966) p. 42.

7. Robert J. List, ed., Smithsonian Meteorological Tables, Smithsonian Miscellaneous Collections, no. 114 (Washington: Smithsonian Institute, 1958), pp. 350-353.

8. Donald E. Kerr, Propagation of Short Radio Waves, Massachusetts Institute of Technology Radiation Laboratory Series, no. 13 (New York: McGraw-Hill Book Company, 1951), p. 396.

9. Ibid., pp. 415-416.

10. Ibid., p. 411.

11. H. Paul Williams, Antenna Theory and Design, Vol. 2: The Electrical Design of Antennae, (London: Sir Isaac Pitman & Sons Ltd., 1966), p. 726.